ACS Catalysis

Research Article

pubs.acs.org/acscatalysis

Understanding Precatalyst Activation in Cross-Coupling Reactions: Alcohol Facilitated Reduction from Pd(II) to Pd(0) in Precatalysts of the Type (η^3-allyl)Pd(L)(Cl) and (η^3-indenyl)Pd(L)(Cl)

Patrick R. Melvin,[†] David Balcells,[‡] Nilay Hazari,*[,†] and Ainara Nova*[,‡]

[†]The Department of Chemistry, Yale University, P.O. Box 208107, New Haven, Connecticut 06520, United States

[‡]Centre for Theoretical and Computational Chemistry (CTCC) and The Department of Chemistry, University of Oslo, P.O. Box 1033, Blindern, 0315 Oslo, Norway

Supporting Information

ABSTRACT: Complexes of the type (η^3-allyl)Pd(L)(Cl) (L = PR_3 or NHC), have been used extensively as precatalysts for cross-coupling and related reactions, with systems containing substituents in the 1-position of the η^3-allyl ligand, such as (η^3-cinnamyl)Pd(L)(Cl), giving the highest activity. Recently, we reported a new precatalyst scaffold based on an η^3-indenyl ligand, (η^3-indenyl)Pd(L)(Cl), which typically provides higher activity than even η^3-cinnamyl supported systems. In particular, precatalysts of the type (η^3-1-^{t}Bu-indenyl)Pd(L)(Cl) give the highest activity. In cross-coupling reactions using this type of Pd(II) precatalyst, it is proposed that the active species is monoligated Pd(0), and the rate of reduction to Pd(0) is crucial. Here, we describe detailed experimental and computational studies which explore the pathway by which the Pd(II) complexes (η^3-allyl)Pd(IPr)(Cl) (IPr = 1,3-bis(2,6-diisopropylphenyl)-1,3-dihydro-2H-imidazol-2-ylidene), (η^3-cinnamyl)Pd(IPr)(Cl), (η^3-indenyl)Pd(IPr)(Cl) and (η^3-1-^{t}Bu-indenyl)Pd(IPr)(Cl) are reduced to Pd(0) in alcoholic solvents, which are commonly used in Suzuki−Miyaura and α-arylation reactions. The rates of reduction for the different precatalysts are compared and we observe significant variability based on the exact reaction conditions. However, in general, η^3-indenyl systems are reduced faster than η^3-allyl systems, and DFT calculations show that this is in part due to the ability of the indenyl ligand to undergo facile ring slippage. Our results are consistent with the η^3-indenyl systems giving increased catalytic activity and provide fundamental information about how to design systems that will rapidly generate monoligated Pd(0) in the presence of alcohols.

Comparison of the rates of Pd(0) formation from Pd(II) precatalysts for cross-coupling

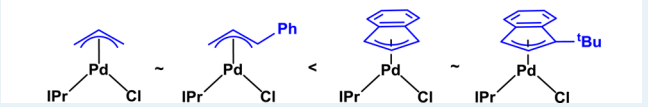

KEYWORDS: *cross-coupling, catalysis, palladium, precatalyst, Suzuki−Miyaura reaction, catalyst activation, DFT calculations*

INTRODUCTION

Palladium-catalyzed cross-coupling is an area of intense research interest because it has numerous applications in the synthesis of pharmaceuticals, fine chemicals, and materials.[1] The most effective cross-coupling catalysts, especially for challenging substrates such as aryl chlorides, are supported by strongly electron-donating and sterically bulky phosphine or N-heterocyclic carbene (NHC) ancillary ligands.[1f,g] The enhanced reactivity of these ligands is attributed to the formation of highly reactive monoligated Pd(0) species.[2] In recent years, a number of well-defined Pd(I) and Pd(II) precatalysts (Figure 1), which are bench stable and readily form monoligated Pd(0) have been developed.[3] A key feature in the effectiveness of these Pd(I) and Pd(II) precatalysts is the rate and efficiency of their conversion into the monoligated Pd(0) active species under the reaction conditions.[1b,f,h] Studies of the mechanism of activation of the Mingos/Hartwig,[4] Buchwald,[3d] and Organ precatalysts[3g,5] have had important implications for the design of improved precatalyst systems.

Recently, it was demonstrated that the efficiency of both Nolan type (η^3-allyl)Pd(NHC)(Cl) and Colacot/Shaughnessy type (η^3-allyl)Pd(PR_3)(Cl) precatalysts is related to two factors: (a) The rate of activation of the ligated Pd(II) precatalyst scaffold to form the catalytically active L-Pd(0) species; and (b) Comproportionation between L-Pd(0) and the starting precatalyst, which forms a Pd(I) μ-allyl dimer of the form (μ-allyl)(μ-Cl)$Pd_2(L)_2$ and removes L-Pd(0) from the reaction mixture.[3m,o,6] Colacot used these results to develop improved precatalysts featuring a 1-methylallyl ligand,[3o] while our group used this information to design a new precatalyst scaffold featuring an η^3-indenyl ligand.[3p] In particular, precatalysts based on the (η^3-1-^{t}Bu-indenyl)Pd(L)(Cl) scaffold were highly active because Pd(I) dimer formation was effectively suppressed. However, surprisingly, given the utility and popularity of catalysts of the type (η^3-allyl)Pd(L)(Cl)[1b,g,3m−o] (L = NHC or PR_3), the mechanism by which Pd(II) is activated to Pd(0) under catalytic conditions is not well understood.[3j,6a,7] In preliminary studies several different reduction pathways have been proposed on the basis of the olefin byproduct observed (Scheme 1): (i) Nucleophilic addition of the base (Nu) to the η^3-allyl ligand, which ultimately generates an olefin of the type CH_2(Nu)−CH═

Received: June 19, 2015
Revised: July 28, 2015
Published: August 17, 2015

DOI: 10.1021/acscatal.5b01291
ACS Catal. 2015, 5, 5596−5606

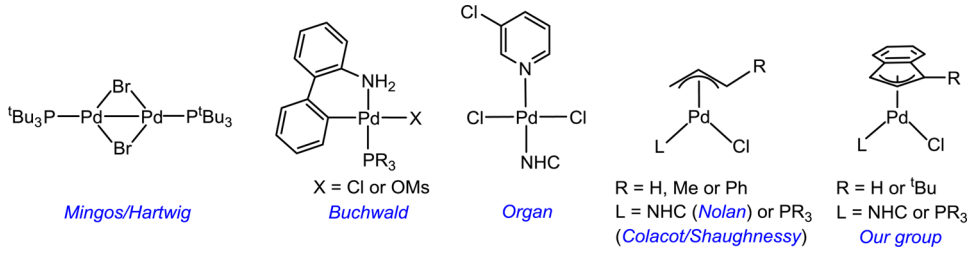

Figure 1. Selection of popular well-defined precatalyst scaffolds with a 1:1 Pd to ligand ratio that are commercially available.

Scheme 1. Mechanisms Proposed for the Reduction of Pd(II) η^3-Allyl Systems with the Experimentally Observed Byproducts Highlighted in Red

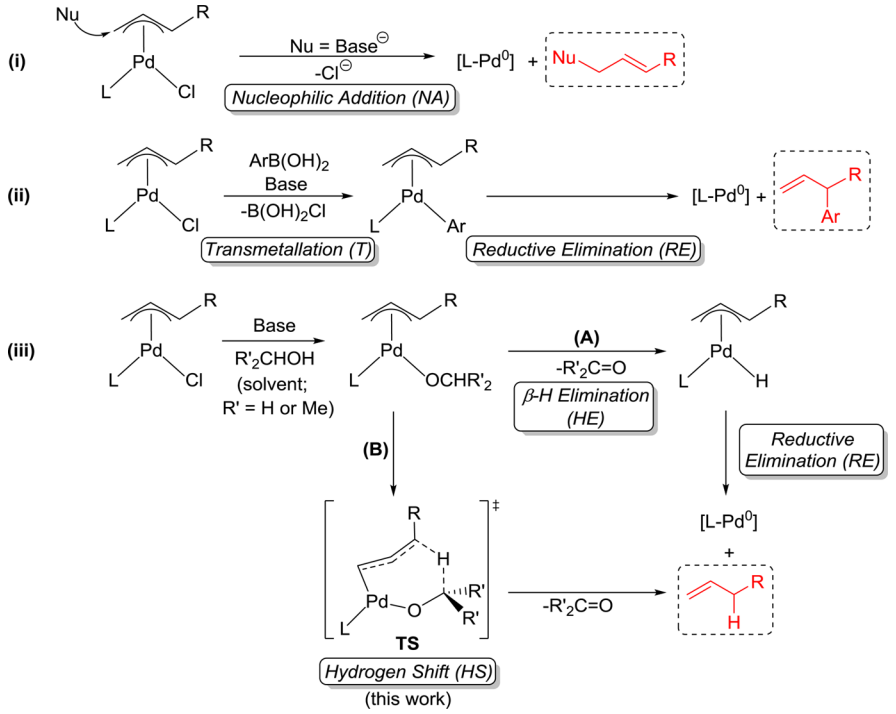

CH(R).[3j,7c] (ii) Transmetalation with the nucleophilic coupling partner such as an aryl (Ar) organoborane in the Suzuki–Miyaura reaction followed by reductive elimination, yielding a CH_2=CH–CH(R) (Ar) olefin;[7b] and (iii) Hydrogen transfer from the alcohol solvents commonly used in Suzuki–Miyaura and α-arylation reactions, yielding a CH_2=CH–CH_2(R) olefin. The latter reaction may be either stepwise (A), by sequential β-H and reductive eliminations,[6a,7a] or concerted (B), by hydrogen shift, as shown by us in this work.

These data suggest that small variations in the nature of the system, including the allyl ligand, the base and the solvent, may result in different reaction mechanisms. In this scenario, it is unclear how the highly active precatalysts based on the η^3-indenyl scaffold are activated. Here, we describe the first comprehensive study, including both experiment and theory, on the activation of (η^3-allyl)Pd(IPr)(Cl) and (η^3-indenyl)Pd-(IPr)(Cl) type precatalysts to Pd(0) in the presence of alcoholic solvents. We demonstrate that η^3-indenyl containing precatalysts activate significantly faster than η^3-allyl systems (Figure 2) and provide a rationalization for these rates on the basis of the hydrogen shift mechanism calculated using DFT.

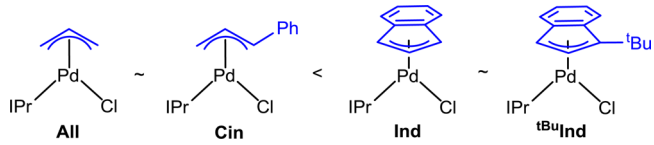

Figure 2. Rates of activation to monoligated Pd(0) for different precatalysts determined experimentally in alcoholic solvents in this work. The pathways of activation which involve a key hydrogen shift are elucidated using DFT calculations.

RESULTS AND DISCUSSION

Experimental Studies of Activation of Pd(II) to Pd(0). The highly active IPr supported precatalysts for the Suzuki-Miyaura reaction **All**, **Cin**, **Ind** and **^{tBu}Ind** were synthesized using literature methods.[3i,l,p] The rates of conversion of the Pd(II) complexes into Pd(0) were studied by treating these compounds with base in the presence of ten equivalents of 1,3-divinyl-1,1,3,3-tetramethyldisiloxane (dvds) and following the reaction using ^{1}H NMR spectroscopy (Table 1). These reactions model the activation of Pd(II) to Pd(0) in catalysis, where oxidative addition to the unstable monoligated Pd(0) complex subsequently occurs to start the catalytic process. In all cases, the products of these reactions are the Pd(0) complex

DOI: 10.1021/acscatal.5b01291
ACS Catal. 2015, 5, 5596–5606

Table 1. Rates of Activation of All, Cin, Ind, or ^{tBu}Ind under Different Conditions in the Presence of dvds[a]

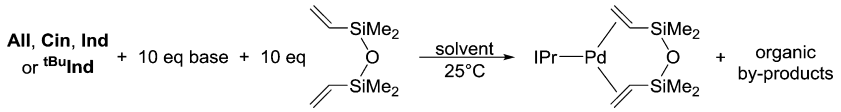

base	solvent	$PhB(OH)_2$ present	rate of activation k_{obs} (s^{-1})[e]			
			All	Cin	Ind	^{tBu}Ind
KO^{t}Bu	d_8-^{i}PrOH[b]	no	$5.6 \pm 0.1 * 10^{-4}$	$3.80 \pm 0.03 * 10^{-3}$	$> 7.7 * 10^{-3}$ ($4.8 \pm 0.1 * 10^{-3}$)[f]	$> 7.7 * 10^{-3}$ ($5.3 \pm 0.2 * 10^{-3}$)[f]
KO^{t}Bu	d_4-MeOH	no	$1.80 \pm 0.02 * 10^{-3}$	$5.1 \pm 0.1 * 10^{-4}$	$> 7.7 * 10^{-3}$ ($5.3 \pm 0.2 * 10^{-3}$)[f]	$> 7.7 * 10^{-3}$ ($5.7 \pm 0.1 * 10^{-3}$)[f]
K_2CO_3	d_4-MeOH[c]	no	$9.6 \pm 0.2 * 10^{-4}$	$4.2 \pm 0.1 * 10^{-4}$	$> 7.7 * 10^{-3}$ ($4.7 \pm 0.1 * 10^{-3}$)[f]	$> 7.7 * 10^{-3}$ ($5.0 \pm 0.2 * 10^{-3}$)[f]
K_2CO_3	d_4-MeOH[c]	yes[d]	$2.4 \pm 0.1 * 10^{-4}$	$1.4 \pm 0.2 * 10^{-4}$	$7.2 \pm 0.1 * 10^{-4}$	$7.6 \pm 0.1 * 10^{-4}$

[a]Reaction conditions: 0.0087 mmol **All**, **Cin**, **Ind**, or ^{tBu}**Ind**, 0.087 mmol of base, 0.087 mmol of dvds in 500 μL of solvent. [b]100 μL of d_8-THF was added along with only 400 μL of ^{i}PrOH. [c]Two equivalents of 18-crown-6 (relative to K_2CO_3) were added to solubilize the K_2CO_3. [d]0.0087 mmol precatalyst, 0.087 mmol phenylboronic acid, 0.096 mmol base, 0.087 mmol dvds in 500 μL d_4-MeOH. [e]All rates are the average of at least two runs and were measured using ^{1}H NMR spectroscopy. [f]The value in brackets is from an experiment performed at 0 °C.

(IPr)Pd(dvds),[8] along with various different organic byproducts. Three different types of reaction conditions, which are relevant to catalysis, were examined. The first set of conditions, which used KO^{t}Bu as the base and d_8-^{i}PrOH as the primary solvent,[9] is similar to the catalytic reaction conditions utilized by Nolan and co-workers.[3l] The second set of conditions using K_2CO_3 and d_4-MeOH as the solvent is related to catalytic reaction conditions that we recently reported.[6a] Under these conditions K_2CO_3 is not soluble and 1,4,7,10,13,16-hexaoxacyclooctadecane (18-crown-6) was used as a solubilizing agent. The third set of reactions, which used KO^{t}Bu as the base and d_4-MeOH as the solvent, was performed as a point of comparison with both the first and second sets of experiments to probe the effect of both solvent and base on the rate of precatalyst activation.

The indenyl complexes **Ind** and ^{tBu}**Ind** were activated the fastest in all cases. In many instances, the activation was so fast that only a minimum rate could be estimated at 25 °C using ^{1}H NMR spectroscopy. A series of reactions analogous to those described in Table 1 at 0 °C, allowed us to establish that ^{tBu}**Ind** activates slightly faster than **Ind**. This is in agreement with the relative catalytic performance of these two complexes[3p] and indicates that modification of the substituent on the indenyl ligand can be used to increase the rate of activation. The cinnamyl species **Cin** was relatively efficiently activated using KO^{t}Bu as the base in d_8-^{i}PrOH, consistent with the excellent catalytic performance of this precatalyst under related reaction conditions.[3l] Although, under these conditions **Cin** activated faster than **All**, **All** was more efficiently activated than **Cin** in both of the reactions conducted in d_4-MeOH. These results indicate that the choice of solvent directly affects the rate of activation and that the optimal solvent for one precatalyst may not be the same as for another precatalyst, even when the precatalysts and solvents are closely related. Finally, the effect of adding phenylboronic acid was also explored and it was observed that it slowed down the rate of activation in all cases. Using K_2CO_3 as the base in d_4-MeOH, in the presence of phenylboronic acid, ^{tBu}**Ind** activates slightly faster than **Ind**.

To gain information about the role of dvds in the activation, reactions were performed in the absence of dvds using the precatalysts **All**, **Cin** and **Ind** (Table 2). In this case, the Pd containing products of the activation of **All**, **Cin** and **Ind** are Pd(I) dimers with bridging allyl or indenyl ligands, which we have previously synthesized and characterized.[6,10] However, the Pd(I) dimers are not soluble under the reaction conditions, which precluded careful kinetic analysis of the data, due to

Table 2. Rates of Activation of All, Cin or Ind under Different Conditions in the Absence of dvds.[a]

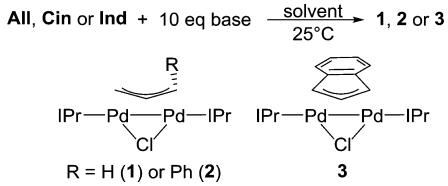

base	solvent	time to completion (minutes)[d]		
		All	Cin	Ind
KO^{t}Bu	d_8-^{i}PrOH[b]	150	90	40
KO^{t}Bu	d_4-MeOH	120	150	30
K_2CO_3[c]	d_4-MeOH	160	180	40

[a]Reaction conditions: 0.0087 mmol **All**, **Cin** or **Ind**, 0.087 mmol of base in 500 μL of solvent. [b]100 μL of d_8-THF was added along with only 400 μL of ^{i}PrOH. [c]Two equivalents of 18-crown-6 (relative to K_2CO_3) were added to solubilize the K_2CO_3. [d]All times to completion are the average of at least two runs and were measured using ^{1}H NMR spectroscopy.

difficulties associated with accurate integration of the ^{1}H NMR spectra. Nevertheless, qualitative analysis indicates that activation experiments performed in the absence of dvds give the same trends as those in the presence of dvds, with the indenyl complex **Ind**, always activating significantly faster than either **All** or **Cin** under all conditions. This suggests that conclusions made about the rate of activation in the presence of dvds are relevant to the true catalytic system which does not contain dvds. It should be noted that the corresponding reactions with ^{tBu}**Ind** did not give clean reactivity, presumably because the Pd(I) dimer with a bridging 1-^{t}Bu-indene ligand is not accessible,[3p] which resulted in a mixture of products being observed.

It was possible to identify the organic byproducts of activation in the presence of dvds using either ^{1}H or ^{13}C NMR spectroscopy (Table 3).[11] Under all conditions, propene, allylbenzene, indene and 1-^{t}Bu-indene were observed as byproducts in activation studies using **All**, **Cin**, **Ind** and ^{tBu}**Ind**, respectively. These species were formed in >95% yield as determined using ^{1}H NMR spectroscopy. In addition, for all reactions performed in ^{i}PrOH, acetone was formed in high yield as determined using ^{13}C NMR spectroscopy. It is proposed that in reactions performed in MeOH, formaldehyde is a byproduct, although it was not directly observed using NMR spectroscopy. Instead resonances consistent with

DOI: 10.1021/acscatal.5b01291
ACS Catal. 2015, 5, 5596−5606

Table 3. Organic Byproducts from Activation of All, Cin, Ind or ^{tBu}Ind under Different Conditions in the Presence of dvds.[a]

base	solvent	$PhB(OH)_2$ present	byproducts from activation: All	Cin	Ind	^{tBu}Ind
KO^{t}Bu	d_8-^{i}PrOH	no	propene, acetone	allylbenzene, acetone	indene, acetone	1-^{t}Bu-indene, acetone
KO^{t}Bu	d_4-MeOH	no	propene, formaldehyde[b]	allylbenzene, formaldehyde[b]	indene, formaldehyde[b]	1-^{t}Bu-indene, formaldehyde[b]
K_2CO_3	d_4-MeOH	no	propene, formaldehyde[b]	allylbenzene, formaldehyde[b]	indene, formaldehyde[b]	1-^{t}Bu-indene, formaldehyde[b]
K_2CO_3	d_4-MeOH	yes	propene, formaldehyde[b]	allylbenzene, formaldehyde[b]	indene, formaldehyde[b]	1-^{t}Bu-indene, formaldehyde[b]

[a]The same reaction conditions described in Table 1 were utilized, with the exception that a mixture of protio and deuterated solvents was utilized to determine the organic byproducts originating from the solvent. [b]Proposed product based on the formation of oligomers of the type $HO(CH_2O)_iCH_3$ ($i > 1$).[12]

oligomers of the type $HO(CH_2O)_iCH_3$ ($i > 1$) were detected,[12] regardless of the choice of base, consistent with the formation of formaldehyde as the initial byproduct in these reactions. The reactions in the presence of phenylboronic acid exhibited the same byproducts, indicating that the **T-RE** mechanism illustrated in Scheme 1 (ii), which involves initial transmetalation of the boronic acid, followed by reductive elimination, is not the major activation pathway. In agreement with this conclusion the expected byproducts from this alternative pathway (for example allylbenzene in the case of **All**) were not detected. For the same reason, the nucleophilic addition mechanism, (i) in Scheme 1, is also excluded. Given

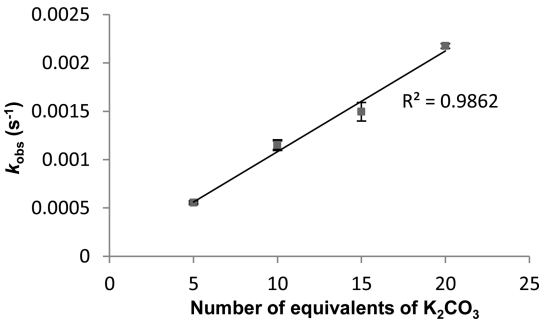

Figure 3. Plot of observed rate constant versus number of equivalents of base for the activation of **All** in d_4-MeOH with K_2CO_3 in the presence of dvds and 18-crown-6 ether measured using ^{1}H NMR spectroscopy.

that activation is first order in base (see Figure 3, for a representative experiment using **All**), we believe that phenylboronic acid inhibits activation by reducing the effective concentration of the base, but does not play a direct role in activation.

DFT Studies of Activation of Pd(II) to Pd(0). Our experimental studies provide the rates of activation of the four systems and the byproduct formed. This allows us to discard mechanisms *i* and *ii* in Scheme 1. However, our mechanistic studies do not provide information about whether the pathway for *iii* is **A** or **B** (Scheme 1). Therefore, DFT calculations were performed to study the elementary steps in the mechanism of activation of **All**, **Cin**, **Ind** and ^{tBu}**Ind** in detail. The calculations were performed using OMe^- as the base, which is equivalent to experiments using KO^{t}Bu as the base in MeOH (Table 1). A number of different pathways were calculated for the activation of all four systems (see Supporting Information). The key intermediates and TS energies for **All** are shown in Schemes 2 and 3, while those for **Cin** and ^{tBu}**In** are shown in Scheme 4. Results for **Ind** are not shown in Schemes but described in the text. Initial substitution of Cl^- by OMe^- can take place via

Scheme 2. Calculated Pathway for the Dissociative and Associative Ligand Substitution of Cl^- by OMe^- in the All System[a]

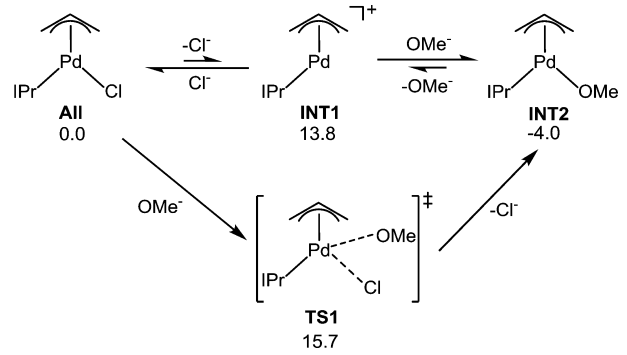

[a]Relative energies are given in kcal mol^{-1}.

dissociative (**INT1** = 13.8 kcal mol^{-1}) or associative (**TS1** = 15.7 kcal mol^{-1}) substitution (Scheme 2). The lower energy barrier for the former process is in agreement with previous experimental studies showing that the addition of excess ^{n}Bu$_4$NCl inhibits activation.[6a] Similar results were obtained for **Cin**, **Ind** and ^{tBu}**Ind**, with larger energy differences between both pathways; 5.3, 5.0, and 9.7 kcal mol^{-1}, respectively, in favor of the dissociative mechanism in all cases.

After the coordination of MeO^-, formation of the olefin observed experimentally requires migration of a proton from the OMe^- group to the allyl ligand. A plausible stepwise mechanism involves β-H elimination followed by reductive elimination of propene (mechanism iii, pathway **A** in Scheme 1). In order to generate the vacant site required for β-H elimination, a change in coordination mode of the allyl ligand from η^3 (**INT2**) to κ^1 (**INT3**) is needed (Scheme 3). This change in coordination mode is endoergic by 10.1 kcal mol^{-1}. The β-H elimination transition state (**TS3**) involves an energy barrier of 24.0 kcal mol^{-1} and connects to a η^2-formaldehyde complex (**INT4**) through a transient agostic intermediate (see Supporting Information). The decoordination of formaldehyde requires a $\eta^2 \rightarrow \kappa^1$ rearrangement, which involves the highest energy transition state found in this pathway; i.e., **TS4**, 28.5 kcal mol^{-1} above reactants. After $\kappa^1 \rightarrow \eta^3$ isomerization of the allyl ligand, reductive elimination takes place through a low energy barrier of 15.1 kcal mol^{-1} (**TS5**) and yields propene. The formation of this product from **INT3** is also possible through the **HS** mechanism, (iii, **B**) in Scheme 1, in which one proton migrates from the MeO^- ligand to the allyl in a single concerted step involving **TS2**, with an energy barrier of 20.5 kcal mol^{-1}. The relaxation of this transition state yields formaldehyde and the Pd(0)-propene complex. The relative

DOI: 10.1021/acscatal.5b01291
ACS Catal. 2015, 5, 5596−5606

Scheme 3. Calculated Pathways for the Activation of All from INT2[a]

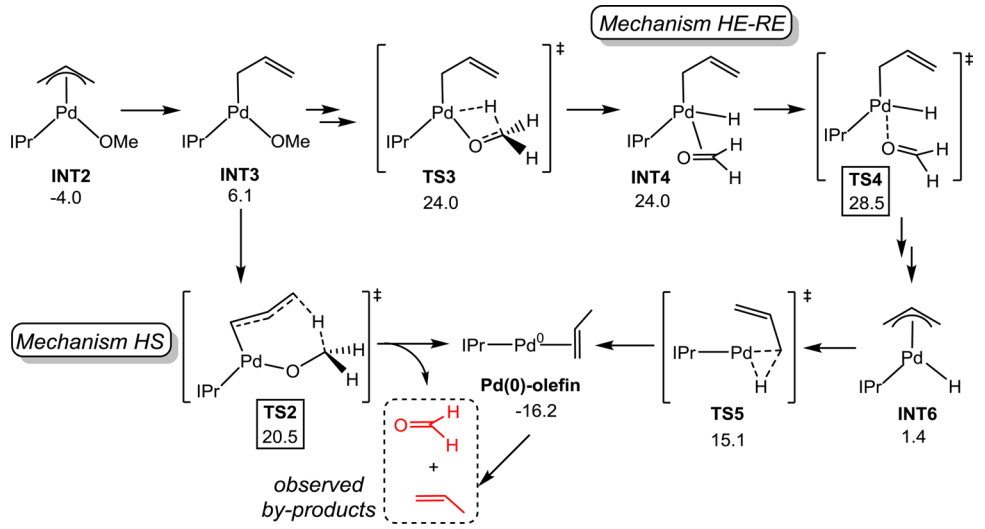

[a]Energies are relative to **All** (Scheme 2) and given in kcal mol^{-1}.

Scheme 4. Calculated Pathways for the Activation of Cin and ^{tBu}Ind from INT2[a]

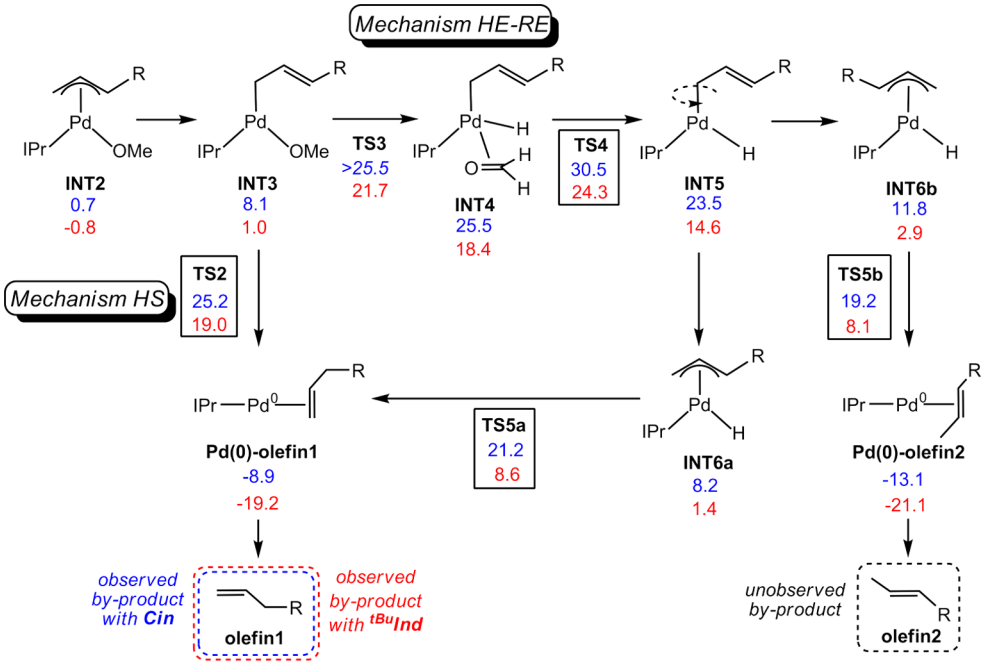

[a]Energies are relative to **Cin** (blue) and ^{tBu}**Ind** (red) and given in kcal mol^{-1}.

energy of **TS2**, which is 8.0 kcal mol^{-1} lower than that of **TS4**, strongly suggests that the **HS** mechanism is kinetically more favorable than the **HE-RE** pathway.

The relative energies of **TS2** and **TS4** were also computed for **Cin**, **Ind** and ^{tBu}**Ind** (see Scheme 4 and S3) and the former is lower in energy in all cases by 5.3, 3.9, and 5.3 kcal mol^{-1}, respectively, showing the same preference for the **HS** mechanism over the **HE-RE** found for **All**. In addition, by computing the reductive elimination step for the unsymmetrical systems **Cin** and ^{tBu}**Ind**, it was found that two transition states (**TS5a** and **TS5b**) are feasible, each one yielding a different Pd(0)-olefin complex with either **olefin1** (terminal; observed) or **olefin2** (internal; not observed). The lower energy of **TS5b** and **Pd(0)-olefin2** with both **Cin** and ^{tBu}**Ind** indicates that **olefin2** would be observed if the **HE-RE** pathway was preferred.[13] The **HS** mechanism is thus supported by both its lower energy barrier and the predicted reaction product, which matches the one observed experimentally.

The energy profiles for the **HS** mechanism with **All**, **Cin**, **Ind** and ^{tBu}**Ind** are given in Scheme 5, showing the rate-limiting barriers; i.e., 24.5, 25.2, 21.7, and 19.8 kcal mol^{-1}, respectively. The barriers correspond to the energy difference between **TS2** and the most stable reactant, which is the starting material for **Cin** and **INT2** for all other systems. Overall, these values are consistent with the experimental trend observed for precatalyst activation rates in MeOH (see Table 1), i.e. ^{tBu}**Ind** > **Ind** > **All** > **Cin**.

DOI: 10.1021/acscatal.5b01291
ACS Catal. 2015, 5, 5596−5606

Scheme 5. Free Energy Profiles (in kcal mol^{-1}) for the Activation of All (black), Cin (red), Ind (green), and ^{tBu}Ind (blue) by a HS Type Mechanism[a]

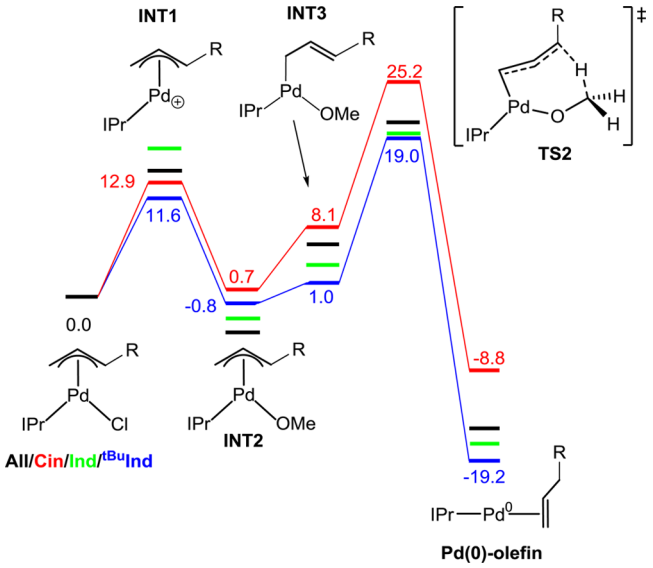

[a]Structures of Indenyl type ligands and energies for **All** and **Ind** have been omitted for clarity.

The structures of the key transition states for activation of **All**, **Cin**, **Ind** and ^{tBu}**Ind** are shown in Figure 4. The structures of the four transition states are similar. In all cases, a seven-membered ring facilitates proton transfer, and the Pd is essentially only bound to one carbon atom of the allyl, cinnamyl, indenyl or 1-^{t}Bu-indenyl ligand. The lowering of the hapticity of those ligands in the transition state is already apparent in **INT3**. Indeed the energy differences between **All**, **Cin**, **Ind** and ^{tBu}**Ind** systems are greater when moving along the reaction coordinate from **INT2** to **INT3** (10.1, 7.3, 5.5, 0.5 kcal mol^{-1}, respectively) than from **INT3** to **TS2** (14.1, 17.1, 16.2, and 17.9 kcal mol^{-1}, respectively). The M-L donor–acceptor interactions in **INT2** and **INT3** were investigated by means of natural bond orbital analysis (NBO version 6).[14] These calculations showed that all systems are stabilized by π-donation, L(π) → Pd(d), between the ligand and the metal center (L = allyl, cinnamyl, indenyl and 1-^{t}Bu-indenyl) in **INT2**. However, this interaction is highly reduced in **INT3**, in agreement with the lowering of the hapticity of L. The natural localized molecular orbitals (NLMOs) associated with this interaction are depicted in Figure 5. In addition to the ligand π-donation to the metal, the NLMOs for **Ind** and ^{tBu}**Ind** show some delocalization of the allyl π-system over the phenyl ring.

Second-order perturbation analysis was carried out to calculate the stabilization energy (SE) of the L(π) → Pd(d) donation for allyl, cinnamyl, indenyl and 1-^{t}Bu-indenyl ligands

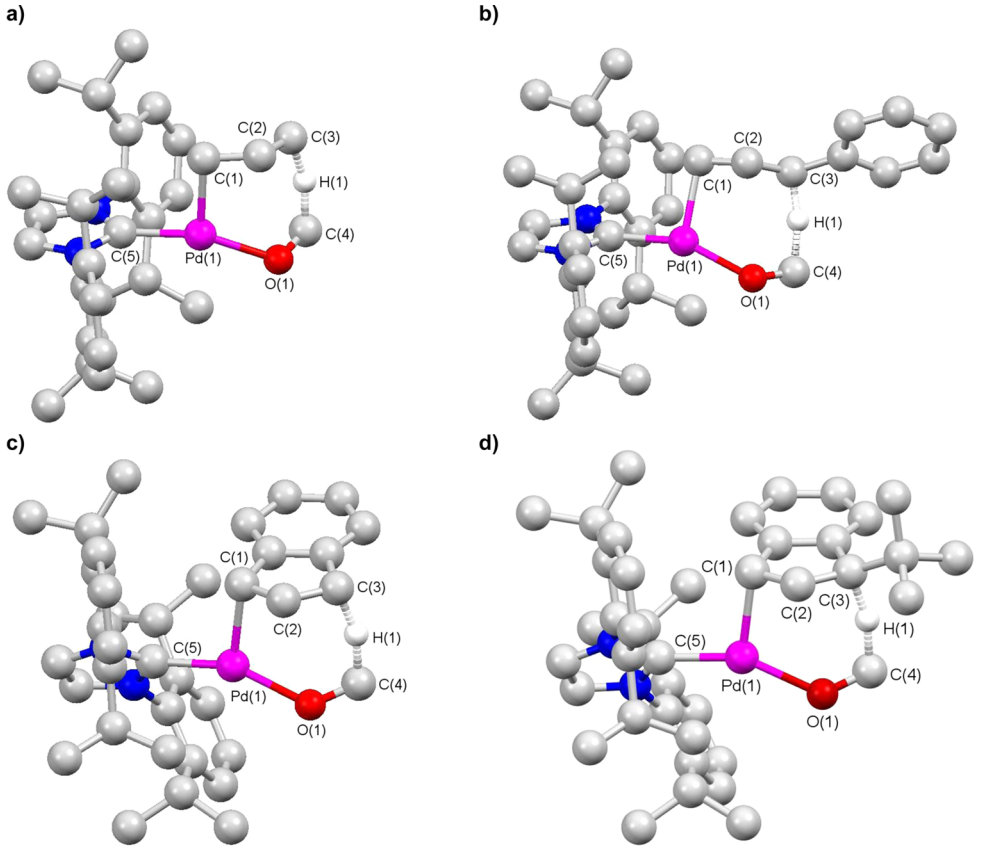

Figure 4. Calculated transition state (**TS2**) structures for activation of (a) **All**, (b) **Cin**, (c) **Ind** and (d) ^{t}**BuInd**. Selected hydrogen atoms are omitted for clarity. Selected bond distances (Å): **a)** Pd(1)–C(1) 2.14, Pd(1)–C(2) 2.67, C(1)–C(2) 1.41, C(2)–C(3) 1.41, C(3)–H(1) 1.36, H(1)–C(4) 1.34, C(4)–O(1) 1.30, Pd(1)–O(1) 2.13, Pd(1)–C(5) 2.02. **b)** Pd(1)–C(1) 2.18, Pd(1)–C(2) 2.71, C(1)–C(2) 1.40, C(2)–C(3) 1.43, C(3)–H(1) 1.30, H(1)–C(4) 1.38, C(4)–O(1) 1.29, Pd(1)–O(1) 2.13, Pd(1)–C(5) 2.03. **c)** Pd(1)–C(1) 2.20, Pd(1)–C(2) 2.74, C(1)–C(2) 1.41, C(2)–C(3) 1.43, C(3)–H(1) 1.33, H(1)–C(4) 1.37, C(4)–O(1) 1.29, Pd(1)–O(1) 2.12, Pd(1)–C(5) 2.05. **d)** Pd(1)–C(1) 2.21, Pd(1)–C(2) 2.75, C(1)–C(2) 1.40, C(2)–C(3) 1.44, C(3)–H(1) 1.33, H(1)–C(4) 1.37, C(4)–O(1) 1.29, Pd(1)–O(1) 2.13, Pd(1)–C(5) 2.05.

DOI: 10.1021/acscatal.5b01291
ACS Catal. 2015, 5, 5596–5606

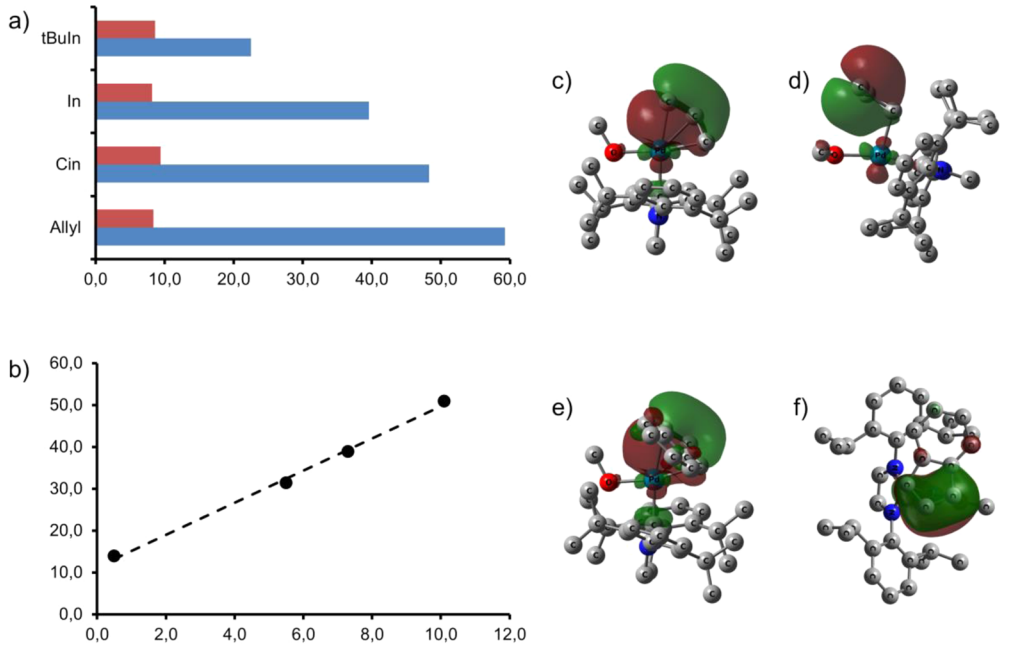

Figure 5. NBO6 analysis: (a) Stabilization energies (x) vs L (y) for **INT2** (blue) and **INT3** (red); (b) Correlation between differences in **INT2**/**INT3** relative energies (x) and stabilization energies (y); natural localized molecular orbitals (NLMOs) for (c) **INT2** (**All**), (d) **INT3** (**All**), (e) **INT2** (**Ind**; side view) and (f) **INT2** (**Ind**; top view). All energies are given in kcal mol^{-1}.

Scheme 6. Proposed Pathway for Activation of All with K2CO3 in MeOH[a]

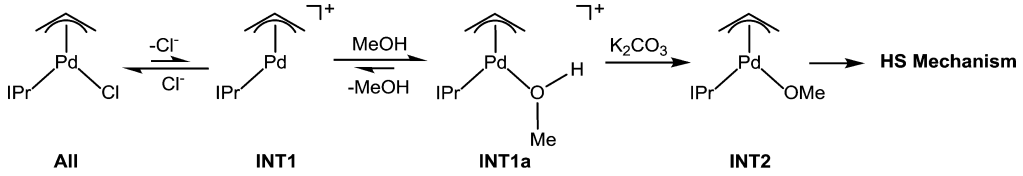

[a]Analogous pathways are proposed for **Cin**, **Ind**, and **^{tBu}Ind**.

in both **INT2** and **INT3**.[15] In line with the different shape of the NLMOs, different SE values for L(π) → Pd(d) were obtained. For **INT2**, SE = 59.3 (**All**), 48.3 (**Cin**), 39.6 (**Ind**) and 22.5 (**^{tBu}Ind**) kcal mol^{-1} (Figure 5 in blue), whereas for **INT3**, SE = 8.4 (**All**), 9.4 (**Cin**), 8.2 (**Ind**) and 8.6 (**^{tBu}Ind**) kcal mol^{-1} (Figure 5 in red). The decrease in the SE values when moving from **All** and **Cin** to **Ind** and **^{tBu}Ind** in **INT2** is consistent with the nature of its NLMOs. The increase in the allyl delocalization by allyl-phenyl conjugation in indenyl type ligands weakens the L(π) → Pd(d) donation in **INT2**. Consequently, the loss in energy expected for the hapticity change from **INT2** to **INT3** is lower for these systems compared to **All** and **Cin**. This result is in agreement with previous studies, which indicate that ring slippage of indenyl ligands coordinated to Pd is facile.[16] The graphic representation of the SE differences for the L(π) → Pd(d) donation in **INT2** and **INT3** versus the energy difference between these two intermediates shows a strong correlation in a linear regression ($y = 3.83x + 11.4$; $r^2 = 0.997$). This supports that the stability of **INT2** relative to **INT3** is largely controlled by the L(π) → Pd(d) donor interaction.

Although our DFT calculations on activation were performed using OMe$^-$ as the base, which is experimentally equivalent to using KO^{t}Bu as the base in MeOH, they can also be related to reactions using K_2CO_3 as the base in MeOH. In this case, K_2CO_3 which is a weak base, is not sufficiently strong to deprotonate MeOH and generate a free MeO$^-$ anion. Therefore, when **All**, **Cin**, **Ind** and **^{tBu}Ind** are activated in MeOH, we propose that MeOH initially coordinates to Pd (**INT1a**) (via dissociative ligand substitution of the Cl$^-$ ligand, **INT1**), which increases its acidity. The coordinated MeOH is subsequently deprotonated by K_2CO_3 to form **INT2**. This pathway is shown for **All** in Scheme 6. We expect that the intermediate **INT1a** and K_2CO_3 are slightly higher in energy than either **All**, **Cin**, **Ind** and **^{tBu}Ind**, MeOH and K_2CO_3, given that no intermediate is observed experimentally. Thus, the energy profile for this reaction will be similar to that calculated for activation using OMe$^-$ as the base, where the energies of the starting materials, **INT2** and **TS2** are crucial. This is consistent with what is observed experimentally where the byproducts and relative rates of activation of **All**, **Cin**, **Ind** and **^{tBu}Ind** using KO^{t}Bu as the base in MeOH are the same as those observed for activation using K_2CO_3 as the base in MeOH.

Experimentally, activation of **Cin** using KO^{t}Bu in ^{i}PrOH is faster than activation of **All**. Under these conditions the primary base in solution is O^{i}Pr$^-$. Given the relatively small calculated difference in energy between $\Delta G^{\ddagger}$ for activation of **All** and **Cin** using OMe$^-$, it is reasonable that changing the base from OMe$^-$ to ^{i}PrO$^-$ could cause a large enough change (~1 kcal mol^{-1}) in the energies of the starting materials, **INT2** or **TS2** to result in **Cin** being easier to activate than **All**. Alternatively, it is possible that there is a different mechanism of activation using O^{i}Pr$^-$. However, given the similar kinetic profile of the reaction

DOI: 10.1021/acscatal.5b01291
ACS Catal. 2015, 5, 5596−5606

and the observation of related byproducts to those found for OMe^-, this seems unlikely.

CONCLUSIONS

In this work, we use both experiment and theory to unambiguously establish the pathway for the activation of the highly active cross-coupling precatalysts **All**, **Cin**, **Ind** and **^{tBu}Ind** in alcoholic solvents, which are commonly used for Suzuki-Miyaura and α-arylation reactions. To our knowledge, this study represents the first comprehensive comparative investigation of precatalyst activation in systems containing allyl and/or indenyl ligands and the mechanistic understanding gained should help with the rational design of improved precatalysts. We show that one reason for the excellent activity of the **^{tBu}Ind** precatalyst is due to its rapid reduction from Pd(II) to Pd(0) under catalytic conditions involving alcoholic solvents. In fact, under these conditions, we estimate that the **^{tBu}Ind** precatalyst activates at least an order of magnitude faster than state of the art **All** and **Cin** precatalysts. This complements previous work which demonstrated that the improved activity of the **^{tBu}Ind** precatalyst compared to **All** and **Cin** precatalysts is in part related to its inability to form a less reactive Pd(I) dimer during catalysis.[6a] DFT calculations suggest that the key step in the activation of **^{tBu}Ind**, as well as the related **All** and **Cin** systems, involves a concerted proton abstraction from a coordinated alkoxide, generated from the alcoholic solvent, by the nucleophilic indenyl or allyl ligand. This process is faster for indenyl ligands compared to allyl ligands primarily due to the ability of the indenyl ligand to undergo facile ring slippage, as evidenced by detailed DFT calculations. The rate of the activation reaction is influenced both by the choice of base and solvent, and these variables should be carefully optimized in catalytic reactions. We believe that the results described in this work with IPr-supported systems will be generalizable to the activation of precatalysts supported by phosphine ligands in alcoholic solvents and in future work we will explore complexes of this type. However, the mechanism of activation of 1-*tert*-butylindenyl scaffolds under conditions which do not involve an alcoholic solvent, such as those used for the Buchwald–Hartwig reaction, remains unclear, and studies are still required to elucidate the pathway of reduction in these cases.

EXPERIMENTAL SECTION

General Methods. Experiments were performed under a dinitrogen atmosphere in an M-Braun drybox or using standard Schlenk techniques unless otherwise stated. Under standard glovebox conditions purging was not performed between uses of pentane, benzene and toluene; thus when any of these solvents were used, traces of all these solvents were in the atmosphere and could be found intermixed in the solvent bottles. Moisture- and air-sensitive liquids were transferred by stainless steel cannula on a Schlenk line or in a drybox. THF was dried by passage through a column of activated alumina followed by storage under dinitrogen. All commercial chemicals were used as received except where noted. MeOH (J. T. Baker) and ^{i}PrOH (Macron Fine Chemicals) were not dried but were degassed by sparging with dinitrogen for 1 h and stored under dinitrogen. Potassium *tert*-butoxide (99.99%, sublimed) was purchased from Aldrich. 2,6-dimethylboronic acid (98%), 1-naphthaleneboronic acid (97%) were purchased from Fisher Scientific. Potassium carbonate was purchased from Mallinckrodt. 1,3-divinyltetramethyldisiloxane was purchased from TCI. Potassium carbonate was ground up with a mortar and pestle and stored in an oven at 130 °C prior to use. Deuterated solvents were obtained from Cambridge Isotope Laboratories. d_4-MeOH, d_8-^{i}PrOH, and d_8-THF were not dried but were degassed prior to use through three freeze–pump–thaw cycles. NMR spectra were recorded on Agilent-400, −500, and −600 spectrometers and Varian-300, −500 spectrometers at ambient probe temperatures unless noted. For variable temperature NMR, the sample temperature was calibrated by measuring the distance between the OH and CH_2 resonances in ethylene glycol (99%, Aldrich). Literature procedures were used to prepare the following compounds: (η^3-allyl)Pd(IPr)(Cl)[3i] (**All**), (η^3-cinnamyl)Pd(IPr)(Cl) (**Cin**),[3l] (η^3-indenyl)Pd(IPr)-(Cl)[3p] (**Ind**) and (η^3-^{t}Bu-indenyl)Pd(IPr)(Cl)[3p] (**^{tBu}Ind**).

Computational Details. All stationary points were fully optimized at the DFT level with the hybrid *meta*-GGA M06 functional[15] including dispersion, as implemented in the Gaussian09 software package (Rev. D.01).[16] Geometry optimizations were carried out on the full system including solvation by MeOH with the continuum SMD model.[17] Frequencies were computed with the aim of classifying all stationary points as either minima (reactants, intermediates and products, with all real frequencies) or saddle points (transition states, with a single imaginary frequency). These calculations were also used to determine the thermochemistry corrections, $(G - E)$, which include the zero-point energies, thermal contributions and entropies. In addition, vibrational data were used to relax the transition states toward the reactants and products connected to them. Two different basis sets were used, BS1, for geometry optimizations and frequency calculations, and BS2, for single-points. BS1 includes polarization functions and small-core pseudopotentials by combining the double-ζ 6-31G** (C, N, O and H)[18] and triple-ζ LANL08* (Pd)[19] basis sets. With BS2, Pd was described at the same level, whereas C, N O and H were described with the triple-ζ 6-311+G** basis set,[20] including polarization and diffuse functions. The single-point calculations were performed at the DFT(M06)/SMD(MeOH)/BS2 level on the DFT-(M06)/SMD(MeOH)/BS1-optimized geometries with the aim of refining the potential energies (E_{sol}). The energies discussed in the text, G_{sol}, were obtained by adding the thermochemistry corrections to the refined potential energies eq 1. The energy correction for a 1 M standard state was also included; i.e. + or −1.9 kcal mol^{-1} for a bimolecular dissociative or associative step, respectively.

$$G_{sol} = E_{sol} + (G - E) + /-1.9 \text{ kcal mol}^{-1} \quad (1)$$

Donor–acceptor interactions were explored by means of natural bond orbital calculations (NBO6 version).[14] The nature of these interactions was determined by computing the associated natural molecular orbitals (NLMO). Second order perturbation analysis was performed to calculate the stabilization energies (SE), which allow for quantifying the relative strength of these interactions.

Experiments on Activation of Pd(II) to Pd(0). *Experimental Details for Table 1: Rates of Activation of **All**, **Cin**, **Ind**, and **^{tBu}Ind** under Different Conditions in the Presence of dvds. d_8-^{i}PrOH/KO^{t}Bu Experiments.* KO^{t}Bu (9.8 mg, 0.087 mmol) was dissolved in 300 μL of d_8-^{i}PrOH along with 100 μL of a 0.87 M solution of dvds in d_8-^{i}PrOH. **All** (5.0 mg), **Cin** (5.6 mg), **Ind** (5.6 mg), or **^{tBu}Ind** (6.0 mg, 0.0087 mmol) was dissolved in 100 μL of d_8-THF. These solutions were combined in a J. Young NMR tube at −78 °C. The

DOI: 10.1021/acscatal.5b01291
ACS Catal. 2015, 5, 5596–5606

reaction mixture was degassed on a Schlenk line, after which dinitrogen was introduced into the NMR tube. An array of ^{1}H NMR spectra was taken at 25 °C (or 0 °C for the cases of **Ind** and **^{tBu}Ind**) over the course of 3 h. During this time, the growth of the methyl protons of the (IPr)Pd(dvds)[8] product were monitored.

d_4-MeOH/KO^{t}Bu Experiments. KO^{t}Bu (9.8 mg, 0.087 mmol) was dissolved in 300 μL of d_4-MeOH along with 100 μL of a 0.87 M solution of dvds in d_4-MeOH. **All** (5.0 mg), **Cin** (5.6 mg), **Ind** (5.6 mg), or **^{tBu}Ind** (6.0 mg, 0.0087 mmol) was dissolved in 100 μL of d_4-MeOH. These solutions were combined in a J. Young NMR tube at −78 °C. The reaction mixture was degassed on a Schlenk line, after which dinitrogen was introduced into the NMR tube. An array of ^{1}H NMR spectra was taken at 25 °C (or 0 °C for the cases of **Ind** and **^{tBu}Ind**) over the course of 3 h. During this time, the growth of the methyl protons of the (IPr)Pd(dvds)[8] product were monitored.

d_4-MeOH/K_2CO_3 Experiments. K_2CO_3 (12.0 mg, 0.087 mmol) and 18-crown-6 ether (46.0 mg, 0.174 mmol) were dissolved in 300 μL of d_4-MeOH along with 100 μL of a 0.87 M solution of dvds in d_4-MeOH. **All** (5.0 mg), **Cin** (5.6 mg), **Ind** (5.6 mg), or **^{tBu}Ind** (6.0 mg, 0.0087 mmol) was dissolved in 100 μL of d_4-MeOH. These solutions were combined in a J. Young NMR tube at −78 °C. The reaction mixture was degassed on a Schlenk line, after which dinitrogen was introduced into the NMR tube. An array of ^{1}H NMR spectra was taken at 25 °C (or 0 °C for the cases of **Ind** and **^{tBu}Ind**) over the course of 3 h. The strong − CH_2 peak from the 18-crown-6 ether was suppressed by presaturating its signal during the experiment. During this time, the growth of the methyl protons of the (IPr)Pd(dvds)[8] product were monitored.

d_4-MeOH/K_2CO_3/PhB(OH)$_2$ Experiments. KO^{t}Bu (10.8 mg, 0.096 mmol) and phenylboronic acid (10.6 mg, 0.087 mmol) were dissolved in 300 μL of d_4-MeOH along with 100 μL of a 0.87 M solution of dvds in d_4-MeOH. **All** (5.0 mg), **Cin** (5.6 mg), **Ind** (5.6 mg), or **^{tBu}Ind** (6.0 mg, 0.0087 mmol) was dissolved in 100 μL of d_4-MeOH. These solutions were combined in a J. Young NMR tube at −78 °C. The reaction mixture was degassed on a Schlenk line, after which dinitrogen was introduced into the NMR tube. An array of ^{1}H NMR spectra was taken at 25 °C over the course of 3 h. During this time, the growth of the methyl protons of the (IPr)Pd(dvds)[8] product were monitored.

*Experimental details for Table 2: Rates of activation of **All**, **Cin** and **^{tBu}Ind** under Different Conditions in the Absence of dvds. d_8-^{i}PrOH/KO^{t}Bu Experiments.* KO^{t}Bu (9.8 mg, 0.087 mmol) was dissolved in 400 μL of d_8-^{i}PrOH. **All** (5.0 mg), **Cin** (5.6 mg), or **Ind** (5.6 mg, 0.0087 mmol) was dissolved in 100 μL of d_8-THF. These solutions were combined in a J. Young NMR tube at −78 °C. The reaction mixture was degassed on a Schlenk line, after which dinitrogen was introduced into the NMR tube. An array of ^{1}H NMR spectra was taken at 25 °C over the course of 3 h. Due to the insolubility of the products, the disappearance of starting Pd(II) precatalyst was monitored to determine the time to completion.

d_4-MeOH/KO^{t}Bu Experiments. KO^{t}Bu (9.8 mg, 0.087 mmol) was dissolved in 400 μL of d_4-MeOH. **All** (5.0 mg), **Cin** (5.6 mg), or **Ind** (5.6 mg, 0.0087 mmol) was dissolved in 100 μL of d_4-MeOH. These solutions were combined in a J. Young NMR tube at −78 °C. The reaction mixture was degassed on a Schlenk line, after which dinitrogen was introduced into the NMR tube. An array of ^{1}H NMR spectra was taken at 25 °C over the course of 3 h. Due to the insolubility of the products, the disappearance of starting Pd(II) precatalyst was monitored to determine the time to completion.

d_4-MeOH/K_2CO_3 Experiments. K_2CO_3 (12.0 mg, 0.087 mmol) and 18-crown-6 ether (46.0 mg, 0.174 mmol) were dissolved in 400 μL of d_4-MeOH. **All** (5.0 mg), **Cin** (5.6 mg), or **Ind** (5.6 mg, 0.0087 mmol) was dissolved in 100 μL of d_4-MeOH. These solutions were combined in a J. Young NMR tube at −78 °C. The reaction mixture was degassed on a Schlenk line, after which dinitrogen was introduced into the NMR tube. An array of ^{1}H NMR spectra was taken at 25 °C over the course of 3 h. The strong − CH_2 peak from the 18-crown-6 ether was suppressed by presaturating its signal during the experiment. Due to the insolubility of the products, the disappearance of starting Pd(II) precatalyst was monitored to determine the time to completion

*Experimental Details for Table 3: Byproducts from Precatalyst Activation of **All**, **Cin**, **Ind**, or **^{tBu}Ind** under Different Conditions in the Presence of dvds. Identifying Propene, Allylbenzene, Indene or 1-^{t}Bu-Indene as Byproducts after Activation Experiments Using Different Reaction Conditions.* K_2CO_3 (12.0 mg, 0.087 mmol) and 18-crown-6 ether (46.0 mg, 0.174 mmol) were dissolved in 300 μL of d_4-MeOH along with 100 μL of a 0.87 M solution of dvds in d_4-MeOH. **All** (5.0 mg, 0.0087 mmol), **Cin** (5.6 mg, 0.0087 mmol) **Ind** (5.6 mg), or **^{tBu}Ind** (6.0 mg, 0.0087 mmol) was dissolved in 100 μL of d_4-MeOH. These solutions were combined in a J. Young NMR tube at −78 °C. The reaction mixture was degassed on a Schlenk line, after which dinitrogen was introduced into the NMR tube. The reaction was allowed to continue at room temperature for 2 h to ensure complete activation of the precatalyst. At this time, a ^{1}H NMR spectrum was recorded. Peaks corresponding to the appropriate by-product were found; a second ^{1}H NMR spectrum was recorded following the addition of a known quantity of the byproduct into the reaction mixture to verify the identity of the organic products produced.

Analogous reactions using d_8-^{i}PrOH as the solvent and KO^{t}Bu as the base and d_4-MeOH as the solvent and KO^{t}Bu as the base were performed using the same method.

Identifying Acetone as a Byproduct after Activation When Using ^{i}PrOH. KO^{t}Bu (9.8 mg, 0.087 mmol) was dissolved in 200 μL of d_8-^{i}PrOH and 200 μL of protio-^{i}PrOH. **All** (5.0 mg, 0.0087 mmol), **Cin** (5.6 mg, 0.0087 mmol) **Ind** (5.6 mg), or **^{tBu}Ind** (6.0 mg, 0.0087 mmol) was dissolved in 100 μL of d_8-THF. These solutions were combined in a J. Young NMR tube at −78 °C. The reaction mixture was degassed on a Schlenk line, after which dinitrogen was introduced into the NMR tube. The reaction was allowed to continue at room temperature for 2 h to ensure complete activation of the precatalyst. At this time, the volatiles were transferred to a new J. Young NMR tube via vacuum transfer using a Schlenk line. A ^{1}H NMR spectrum was recorded and peaks with chemical shifts corresponding to acetone were identified.

Identifying Formaldehyde as a Byproduct after Activation Using MeOH. K_2CO_3 (12.0 mg, 0.087 mmol) and 18-crown-6 ether (46.0 mg, 0.174 mmol) were dissolved in 200 μL of d_4-MeOH and 200 μL of protio-MeOH. **All** (5.0 mg, 0.0087 mmol), **Cin** (5.6 mg, 0.0087 mmol) **Ind** (5.6 mg), or **^{tBu}Ind** (6.0 mg, 0.0087 mmol) was dissolved in 100 μL of d_4-MeOH. These solutions were combined in a J. Young NMR tube at −78 °C. The reaction mixture was degassed on a Schlenk line, after which dinitrogen was introduced into the NMR tube. The

DOI: 10.1021/acscatal.5b01291
ACS Catal. 2015, 5, 5596−5606

reaction was allowed to continue at room temperature for 2 h to ensure complete activation of the precatalyst. At this time, the volatiles were transferred to a new J. Young NMR tube via vacuum transfer using a Schlenk line. Peaks corresponding to the hemiacetal products reported by Hahnenstein et al. for formaldehyde in MeOH were observed.[12]

■ ASSOCIATED CONTENT

Supporting Information

The Supporting Information is available free of charge on the ACS Publications website at DOI: 10.1021/acscatal.5b01291.

Further experimental details and details of DFT calculations (PDF)

■ AUTHOR INFORMATION

Corresponding Authors

*E-mail: nilay.hazari@yale.edu.
*E-mail: ainara.nova@kjemi.uio.no.

Notes

The authors declare no competing financial interest.

■ ACKNOWLEDGMENTS

AN and DB acknowledge support from the Norwegian Research Council through the Center of Excellence for Theoretical and Computational Chemistry (CTCC) (Grant No. 179568/V30) and the Norwegian Metacenter for Computational Science (NOTUR; Grant nn4654k). DB also thanks the EU REA for a Marie Curie Fellowship (Grant CompuWOC/618303). PRM thanks the NSF for support as NSF Graduate Research Fellows. NH is a fellow of the Alfred P. Sloan Foundation and a Camille and Henry-Dreyfus Foundation Teacher Scholar.

■ REFERENCES

(1) (a) Hartwig, J. F. *Acc. Chem. Res.* **2008**, *41*, 1534−1544. (b) Marion, N.; Nolan, S. P. *Acc. Chem. Res.* **2008**, *41*, 1440−1449. (c) Fu, G. C. *Acc. Chem. Res.* **2008**, *41*, 1555−1564. (d) Würtz, S.; Glorius, F. *Acc. Chem. Res.* **2008**, *41*, 1523−1533. (e) Martin, R.; Buchwald, S. L. *Acc. Chem. Res.* **2008**, *41*, 1461−1473. (f) Johansson Seechurn, C. C. C.; Kitching, M. O.; Colacot, T. J.; Snieckus, V. *Angew. Chem., Int. Ed.* **2012**, *51*, 5062−5085. (g) Li, H.; Johansson Seechurn, C. C. C.; Colacot, T. J. *ACS Catal.* **2012**, *2*, 1147−1164. (h) Valente, C.; Calimsiz, S.; Hoi, K. H.; Mallik, D.; Sayah, M.; Organ, M. G. *Angew. Chem., Int. Ed.* **2012**, *51*, 3314−3332. (i) *New Trends in Cross-Coupling: Theory and Applications*. RSC Catalysis Series No. 21; Colacot, T. J, Ed.; The Royal Society of Chemistry: Cambridge, U.K., 2015; pp 1−864.

(2) Christmann, U.; Vilar, R. *Angew. Chem., Int. Ed.* **2005**, *44*, 366−374.

(3) (a) Vilar, R.; Mingos, D. M. P.; Cardin, C. J. *J. Chem. Soc., Dalton Trans.* **1996**, 4313−4314. (b) Stambuli, J. P.; Kuwano, R.; Hartwig, J. F. *Angew. Chem., Int. Ed.* **2002**, *41*, 4746−4748. (c) Biscoe, M. R.; Fors, B. P.; Buchwald, S. L. *J. Am. Chem. Soc.* **2008**, *130*, 6686−6687. (d) Kinzel, T.; Zhang, Y.; Buchwald, S. L. *J. Am. Chem. Soc.* **2010**, *132*, 14073−14075. (e) Bruno, N. C.; Tudge, M. T.; Buchwald, S. L. *Chem. Sci.* **2013**, *4*, 916−920. (f) O'Brien, C. J.; Kantchev, E. A. B.; Valente, C.; Hadei, N.; Chass, G. A.; Lough, A.; Hopkinson, A. C.; Organ, M. G. *Chem. - Eur. J.* **2006**, *12*, 4743−4748. (g) Organ, M. G.; Chass, G. A.; Fang, D.-C.; Hopkinson, A. C.; Valente, C. *Synthesis* **2008**, *2008*, 2776−2797. (h) Nasielski, J.; Hadei, N.; Achonduh, G.; Kantchev, E. A. B.; O'Brien, C. J.; Lough, A.; Organ, M. G. *Chem. - Eur. J.* **2010**, *16*, 10844−10853. (i) Viciu, M. S.; Germaneau, R. F.; Nolan, S. P. *Org. Lett.* **2002**, *4*, 4053−4056. (j) Viciu, M. S.; Germaneau, R. F.; Navarro-Fernandez, O.; Stevens, E. D.; Nolan, S. P. *Organometallics* **2002**, *21*, 5470−5472. (k) Navarro, O.; Kaur, H.; Mahjoor, P.; Nolan, S. P. *J. Org. Chem.* **2004**, *69*, 3173−3180. (l) Marion, N.; Navarro, O.; Mei, J.; Stevens, E. D.; Scott, N. M.; Nolan, S. P. *J. Am. Chem. Soc.* **2006**, *128*, 4101−4111. (m) Hill, L. L.; Crowell, J. L.; Tutwiler, S. L.; Massie, N. L.; Hines, C. C.; Griffin, S. T.; Rogers, R. D.; Shaughnessy, K. H.; Grasa, G. A.; Johansson Seechurn, C. C. C.; Li, H.; Colacot, T. J.; Chou, J.; Woltermann, C. J. *J. Org. Chem.* **2010**, *75*, 6477−6488. (n) Johansson Seechurn, C. C. C.; Parisel, S. L.; Colacot, T. J. *J. Org. Chem.* **2011**, *76*, 7918−7932. (o) DeAngelis, A. J.; Gildner, P. G.; Chow, R.; Colacot, T. J. *J. Org. Chem.* **2015**, *80*, 6794−6813. (p) Melvin, P. R.; Nova, A.; Balcells, D.; Dai, W.; Hazari, N.; Hruszkewycz, D. P.; Shah, H. P.; Tudge, M. T. *ACS Catal.* **2015**, *5*, 3680−3688.

(4) Proutiere, F.; Aufiero, M.; Schoenebeck, F. *J. Am. Chem. Soc.* **2012**, *134*, 606−612.

(5) (a) Nasielski, J.; Hadei, N.; Achonduh, G.; Kantchev, E. A. B.; O'Brien, C. J.; Lough, A.; Organ, M. G. *Chem. - Eur. J.* **2010**, *16*, 10844−10853. (b) Sayah, M.; Lough, A. J.; Organ, M. G. *Chem. - Eur. J.* **2013**, *19*, 2749−2756.

(6) (a) Hruszkewycz, D. P.; Balcells, D.; Guard, L. M.; Hazari, N.; Tilset, M. *J. Am. Chem. Soc.* **2014**, *136*, 7300−7316. (b) Hruszkewycz, D. P.; Guard, L. M.; Balcells, D.; Hazari, N.; Feldman, N.; Tilset, M. *Organometallics* **2015**, *34*, 381−394.

(7) (a) Fantasia, S.; Nolan, S. P. *Chem. - Eur. J.* **2008**, *14*, 6987−6993. (b) Ortiz, D.; Blug, M.; Le Goff, X.-F.; Le Floch, P.; Mezailles, N.; Maître, P. *Organometallics* **2012**, *31*, 5975−5978. (c) Borjian, S.; Baird, M. C. *Organometallics* **2014**, *33*, 3936−3940.

(8) Jackstell, R.; Harkal, S.; Jiao, H.; Spannenberg, A.; Borgmann, C.; Röttger, D.; Nierlich, F.; Elliot, M.; Niven, S.; Cavell, K.; Navarro, O.; Viciu, M. S.; Nolan, S. P.; Beller, M. *Chem. - Eur. J.* **2004**, *10*, 3891−3900.

(9) A small amount of d_8-THF was also added to ensure homogeneous reaction conditions.

(10) (a) Hruszkewycz, D. P.; Wu, J.; Hazari, N.; Incarvito, C. D. *J. Am. Chem. Soc.* **2011**, *133*, 3280−3283. (b) Hruszkewycz, D. P.; Wu, J.; Green, J. C.; Hazari, N.; Schmeier, T. J. *Organometallics* **2012**, *31*, 470−485. (c) Dai, W.; Chalkley, M. J.; Brudvig, G. W.; Hazari, N.; Melvin, P. R.; Pokhrel, R.; Takase, M. K. *Organometallics* **2013**, *32*, 5114−5127.

(11) The organic byproducts detected in the absence of dvds are the same as those observed in the presence of dvds.

(12) Hahnenstein, I.; Hasse, H.; Kreiter, C. G.; Maurer, G. *Ind. Eng. Chem. Res.* **1994**, *33*, 1022−1029.

(13) We suggest that the observation of the product Nu(CH_2CH═CHR) in ref 7c (i in Scheme 1) is indicative of the preferred formation of olefin2 when a RE pathway is preferred, because in this case the NA mechanism probably starts by ligand substitution of Cl^- by Nu followed by RE.

(14) Glendening, E. D.; Landis, C. R.; Weinhold, F. *J. Comput. Chem.* **2013**, *34*, 1429−1437.

(15) (a) Zhao, Y.; Truhlar, D. G. *Theor. Chem. Acc.* **2008**, *120*, 215−241. (b) Zhao, Y.; Truhlar, D. G. *Acc. Chem. Res.* **2008**, *41*, 157−167.

(16) Frisch, M. J.; Trucks, G. W.; Schlegel, H. B.; Scuseria, G. E.; Robb, M. A.; Cheeseman, J. R.; Scalmani, G.; Barone, V.; Mennucci, B.; Petersson, G. A.; Nakatsuji, H.; Caricato, M.; Li, X.; Hratchian, H. P.; Izmaylov, A. F.; Bloino, J.; Zheng, G.; Sonnenberg, J. L.; Hada, M.; Ehara, M.; Toyota, K.; Fukuda, R.; Hasegawa, J.; Ishida, M.; Nakajima, T.; Honda, Y.; Kitao, O.; Nakai, H.; Vreven, T.; Montgomery, Jr., J. A.; Peralta, J. E.; Ogliaro, F.; Bearpark, M.; Heyd, J. J.; Brothers, E.; Kudin, K. N.; Staroverov, V. N.; Kobayashi, R.; Normand, J.; Raghavachari, K.; Rendell, A.; Burant, J. C.; Iyengar, S. S.; Tomasi, J.; Cossi, M.; Rega, N.; Millam, N. J.; Klene, M.; Knox, J. E.; Cross, J. B.; Bakken, V.; Adamo, C.; Jaramillo, J.; Gomperts, R.; Stratmann, R. E.; Yazyev, O.; Austin, A. J.; Cammi, R.; Pomelli, C.; Ochterski, J. W.; Martin, R. L.; Morokuma, K.; Zakrzewski, V. G.; Voth, G. A.; Salvador, P.; Dannenberg, J. J.; Dapprich, S.; Daniels, A. D.; Farkas, Ö.; Foresman, J. B.; Ortiz, J. V.; Cioslowski, J.; Fox, D. J. *Gaussian 09*, Revision D.01; Gaussian, Inc.: Wallingford CT, 2009.

DOI: 10.1021/acscatal.5b01291
ACS Catal. 2015, 5, 5596−5606

(17) Marenich, A. V.; Cramer, C. J.; Truhlar, D. G. *J. Phys. Chem. B* **2009**, *113*, 6378−6396.
(18) Hehre, W. J.; Ditchfield, R.; Pople, J. A. *J. Chem. Phys.* **1972**, *56*, 2257−2261.
(19) Roy, L. E.; Hay, P. J.; Martin, R. L. *J. Chem. Theory Comput.* **2008**, *4*, 1029−1031.
(20) (a) McLean, A. D.; Chandler, G. S. *J. Chem. Phys.* **1980**, *72*, 5639−5648. (b) Krishnan, R.; Binkley, J. S.; Seeger, R.; Pople, J. A. *J. Chem. Phys.* **1980**, *72*, 650−654.

DOI: 10.1021/acscatal.5b01291
ACS Catal. 2015, 5, 5596−5606